Available online at www.sciencedirect.com

ScienceDirect

journal homepage: http://www.elsevier.com/locate/rpor

Original research article

Synthesis, quality control and determination of metallic impurities in ^{18}F-fludeoxyglucose production process

Krzysztof Kilian[b,*], *Bartłomiej Chabecki*[a], *Justyna Kiec*[a], *Agnieszka Kunka*[a], *Barbara Panas*[a], *Maciej Wójcik*[a], *Anna Pękal*[b]

[a] *University of Warsaw, Department of Physics, Hoża 69, 00-681 Warsaw, Poland*
[b] *University of Warsaw, Heavy Ion Laboratory, Pasteur 5a, 02-093 Warsaw, Poland*

ARTICLE INFO

Article history:
Received 16 September 2013
Received in revised form
15 February 2014
Accepted 11 March 2014

Keywords:
^{18}FDG
Radionuclidic impurities
Radiopharmaceuticals
Gamma-spectrometry

ABSTRACT

Aim: The aim of this study was to synthesize ^{18}FDG in some consecutive runs and check the quality of manufactured radiopharmaceuticals and to determine the distribution of metallic impurities in the synthesis process.
Background: For radiopharmaceuticals the general requirements are listed in European Pharmacopeia and these parameters have to be checked before application for human use.
Materials and methods: Standard methods for the determination of basic characteristics of radiopharmaceuticals were used. Additionally, high resolution γ spectrometry was used for the assessment of nuclidic purity and inductively coupled plasma with mass spectrometry to evaluate metallic content.
Results: Results showed sources and distribution of metallic and radiometallic impurities in the production process. Main part is trapped in the initial separation column of the synthesis unit and is not distributed to the final product in significant amounts.
Conclusions: Produced ^{18}FDG filled requirements of Ph.Eur. and the content of radionuclidic and metallic impurities was in the acceptable range.

1. Background

Positron emission tomography (PET) is a dynamically developing imaging method of nuclear medicine, which allows to diagnose metabolic changes in human body. PET diagnostic techniques use β+ emitting isotopes for labeling biologically active compounds and track their distribution in a living organism. Due to its relatively long half-life (110 min), ^{18}F is the most commonly used radioisotope in PET and is produced in medical cyclotrons (mostly proton-deuteron 10–20 MeV machines). Nowadays, the most widely used radiopharmaceutical for diagnostic procedures using PET is ^{18}FDG, the glucose derivative labeled with ^{18}F, which applications are regularly reviewed[1–7] and standardized.[8]

* *Corresponding author at*: Heavy Ion Laboratory, University of Warsaw, Pasteur 5a, 02093 Warsaw, Poland. Tel.: +48 22 55 46 214.
E-mail address: kilian@slcj.uw.edu.pl (K. Kilian).
http://dx.doi.org/10.1016/j.rpor.2014.03.001

2. Aim

One of the most important aspects of working with ^{18}FDG is a short time (about 30 min) that can be spent on quality control and release procedures, thus the speed, simplicity and reliability of developed analytical methods are critical factors. For radiopharmaceuticals, the general requirements are listed in European Pharmacopoeia[9] and these parameters have to be checked before application for human use. Short-lived radiopharmaceutical preparations may be released before completion of some tests, specified in individual monographs. The aim of this study was to synthesize ^{18}F-FDG in some consecutive runs and check the quality of manufactured radiopharmaceuticals. Several tests were performed to determine chemical and radiochemical impurities, chemical identity and other adequate parameters for parenteral formulation. During production process, trace amounts of metallic radioisotopes are produced due to radio activation on the metal target housing. In addition, the distribution of metallic impurities on synthesis and dispensing module was measured by gamma spectroscopy and level of non-radioactive metals was determined with inductively coupled plasma with mass spectrometry (ICP-MS).

3. Materials and methods

3.1. ^{18}FDG manufacturing

^{18}FDG was synthesized in six independent runs with standard method from mannose triflate with alkaline hydrolysis as initially proposed in Ref. 10. Cyclotron GE PETtrace840 with high yield niobium target (General Electric, Uppsala, Sweden) was the source of anionic fluorine. Standard produced activity in ^{18}O(p,n)^{18}F reaction with 16.5 MeV proton beam at 40–45 μA, was 4.0 ± 0.2 Ci (140.6–155.4 GBq) after 120 min of irradiation and was transferred to the GE MX_{FDG} unit (General Electric, Liege, Belgium), where the synthesis and purification were performed. In the synthesis path, the ^{18}F-fluoride solution was passed through an ion exchange column, which trapped anions. Cations, including some metal contaminants, were collected with the recovered enriched water. [^{18}F]fluoride was then eluted to the reaction vessel with a mixture of potassium carbonate and Kryptofix 2.2.2, then water was removed by azeotropic distillation with acetonitrile and ^{18}F reacted with mannose triflate. After alkaline hydrolysis, the solution was purified with sequence of C18-RP and alumina columns and eluted with water. The final product was formulated with saline, passed through a 0.22 μm filter and dispensed in automatic module DDS-Vials (Tema-Synergie, Italy). Starting materials were, ready-to-use, Ph.Eur. compliant kits, obtained from ABX (Radeberg, Germany).

3.2. Identification

Identification tests were performed as described in Ref. 9. For γ-spectrometry, high resolution germanium detector GMX-20190-P with digital signal processor (DSPEC, Ortec) and GammaVison software was used. 2 μL sample was applied on silica plate, fixed in a holder and inserted into a 5 cm Pb shielded, low-background housing. Spectra was recorded for 5 min.

Half-life was measured with Atomlab300 (Biodex, USA) dose calibrator: 300 μL (1.2–1.5 GBq) sample was crimped in penicillin vial, fixed in a standard vial holder and measured in triplicate at 20 min intervals.

Identity of manufactured ^{18}FDG was confirmed by comparison of retention time to the certified reference standard (CRS) of main compound (ABX, Radeberg, Germany).

3.3. Radionuclidic purity

Radionuclidic purity and radionuclidic impurities were determined using gamma spectroscopy with a high resolution germanium detector GMX-20190-P with a digital signal processor (DSPEC, Ortec) with GammaVison software. Efficiency and energy calibration was performed with ^{241}Am (255.162 kBq at the day of measurements), ^{137}Cs (203.425 kBq at the day of measurements) and ^{152}Eu (260.733 kBq at the day of measurements) sources at 13.9, 17.8, 26.47, 59.67, 121.9, 244.8, 344.37, 661.7, 788.98, 964.13, 1085.92, 1112.17 and 1408.14 keV, respectively. For sources and samples, a universal holder, fixed in 14 cm from a detector window was constructed and located in a fully shielded (5 cm Pb) low-background housing.

The spectra were recorded in 10,800 s each for final product and purification cartridges used during the synthesis of 2-[^{18}F]FDG: ion exchange columns Accel Plus QMA Sep-Pak™, used for preconcentration and separation of ^{18}F from target, reverse phase separation columns Sep-Pak™ C-18 RP used in a basic hydrolysis and purification process of FDG, alumina columns Sep-PakTM N Plus for ionic contaminants removal. Isotopes were identified on the basis of the characteristic γ-emissions. Only for final determination of impurities in ^{18}FDG, the time was extended to 21,600 s. Each peak was analyzed by marking the region of interest and recording the energy, count rate and background corrected area.

The γ-ray spectra for radionuclidic purity test A was recorded immediately after synthesis and test B was performed 24 h after irradiation. Recorded activities were calibrated at the end of synthesis (EOS).

The γ-ray spectra of the residual radionuclides were collected 72 h (36 times the ^{18}F half-life) after irradiation, because by that time the ^{18}F activity decreased to a level comparable to longer-lived compounds and did not hamper the spectra recording.

3.4. Radiochemical purity

Radiochemical purity (test A) was performed with an ion chromatography system ICS-5000+ (Thermo Scientific, former Dionex) with a pulsed amperometric detector and radiometric detector (GabiStar, Raytest, Germany). 20 μL sample was injected via a manual multiport valve. The separation was done on Thermo Scientific Carbopac PA-10 column (250 mm × 4.0 mm i.d., 10 μm), with 0.1 M NaOH (CO_2-free) as a mobile phase and 1 mL/min flow rate. Data acquisition and processing was preformed with Chromeleon software.

Radiochemical purity determination (test B) was conducted with a thin layer chromatography system Bioscan

MiniScan B-MS-100 (Canberra Packard) with Flow-count B-FC-100 (Canberra Packard) data processing unit. 2 μL of sample were introduced on a silica gel plate and developed on 8 cm path in a 95:5 acetonitrile–water mixture.

To ensure the quality of measurements, methods were developed and validated with certified reference standards (CRS) of main compound and impurities.

3.4.1. *Isotonicity and pH*

Isotonicity was determined by cryogenic osmometer (Knauer, Germany) in 50 μL samples. Measurements of pH were conducted with MulitiSeven pH-meter (Mettler-Toledo, Germany) with microelectrode vs. 4.01, 7.01 and 9.21 buffers (Hamilton, UK).

3.4.2. *Kryptofix content*

Since the 7th edition the Ph.Eur has replaced in fludeoxyglucose monograph thin-layer chromatographic (TLC) detection of Kryptofix 2.2.2 with the simple color spot test.[11] Silica gel stripes, immersed in iodoplatinate reagent were used for optical comparison of color reaction versus pattern (blank, saline, sample, positive sample) with pass/fail criteria.

3.4.3. *Residual organic solvents content*

Head-space gas chromatography was performed on 7890A Agilent system, equipped with a J&W HP-5 column (30 m × 0.32 mm × 0.25 μm) and a flame ionization detector (FID). GC system was supplied with an H2 (30 mL/min) from CFH200 generator (Peak Scientific, UK), ensuring 99.9995% of hydrogen purity, zero-air (400 mL/min) from a Jun-Air 0F301-4B generator (Jun-Air, UK) and He (6.0, Air Products, flow rate 25 mL/min). Gas chromatographic system was operated at the following conditions: oven temperature 40 °C for 1 min, inlet temperature 150 °C, detector temperature 180 °C.

The samples were injected via 7694E Agilent head-space system. For a comfortable sample application, 5-microliter single-use capillaries (Drummond Scientific, USA) were used for transfer the radioactive sample to 10 mL penicillin vials with aluminum caps and PTFE/Si septa (Agilent). Head-space injector was set to 80 °C for 2 min, then sample was equilibrated for 0.2 min and transferred to the GC system. The loop and transfer line were heated to 105 °C and 110 °C, respectively. Chemstation software was used for operation of chromatograph, acquisition and processing of data.

3.5. *Sterility and bacterial endotoxins*

Sterility test was performed by an external microbial laboratory as specified in Ref. 9. For bacterial endotoxins the gel-clot method (limit test) was used, where gel formation indicated the presence of endotoxins. The test was performed with Pyrogent™ set (Lonza, Belgium) The gel formation in sequence of samples (blank, sample, water spiked with endotoxins, spiked sample) after 1 h incubation at 37 °C was inspected manually.

3.6. *Heavy metals determination*

Inductively coupled plasma with mass spectrometry (ICP-MS, Perkin Elmer Elan 9000) was used for the determination of Cu,

Table 1 – Identified radionuclides and their activity in the recovered ^{18}O water and columns along the ^{18}FDG synthesis process.

Radionuclide	Reaction	Water average [Bq]	QMA average [Bq]	QMA range [Bq]	C18 (1) [Bq]	C18 (2) [Bq]	Alumina [Bq]	^{18}FDG [Bq]
^{7}Be	$^{10}B(p,\alpha)$	N/d	187	99–348	N/d	N/d	N/d	N/d
^{51}Cr	$^{52}Cr(p,pn)^{51}Cr^{50}Cr(n,\gamma)$	10	177	82–346	<5	<5	<5	<2
^{48}V	$^{48}Ti(p,n)$	N/d	44	20–65	N/d	N/d	N/d	N/d
^{52}Mn	$^{52}Cr(p,n)$	247	141	46–232	<5	<5	<5	<2
^{55}Co	$^{56}Fe(p,2n)$	N/d	85	65–110	N/d	N/d	N/d	N/d
^{56}Co	$^{56}Fe(p,n)$	260	532	350–775	<5	<5	<5	<2
^{56}Ni	$^{54}Fe(\alpha, 2n)$ $^{56}Co(p,n)$	N/d	412	312–647	N/d	N/d	N/d	N/d
^{57}Co	$^{56}Fe(p, \gamma)$	219	27	N/d–45	N/d	N/d	N/d	N/d
^{54}Mn	$^{54}Cr(p,n)$	45	10	N/d–28	N/d	N/d	N/d	N/d
^{58}Co	$^{58}Ni(n,p)$	608	145	65–298	N/d	N/d	N/d	N/d
^{95m}Tc	$^{95}Mo(p,n)$	N/d	52	36–78	N/d	N/d	N/d	N/d
^{96}Tc	$^{96}Mo(p,n)$	N/d	1251	675–1889	N/d	N/d	N/d	N/d
^{182}Re	$^{182}W(p,n)$	N/d	34	N/d–65	N/d	N/d	N/d	N/d
^{183}Re	$^{183}W(p,n)$	N/d	25	N/d–48	N/d	N/d	N/d	N/d

N/d: not detected.

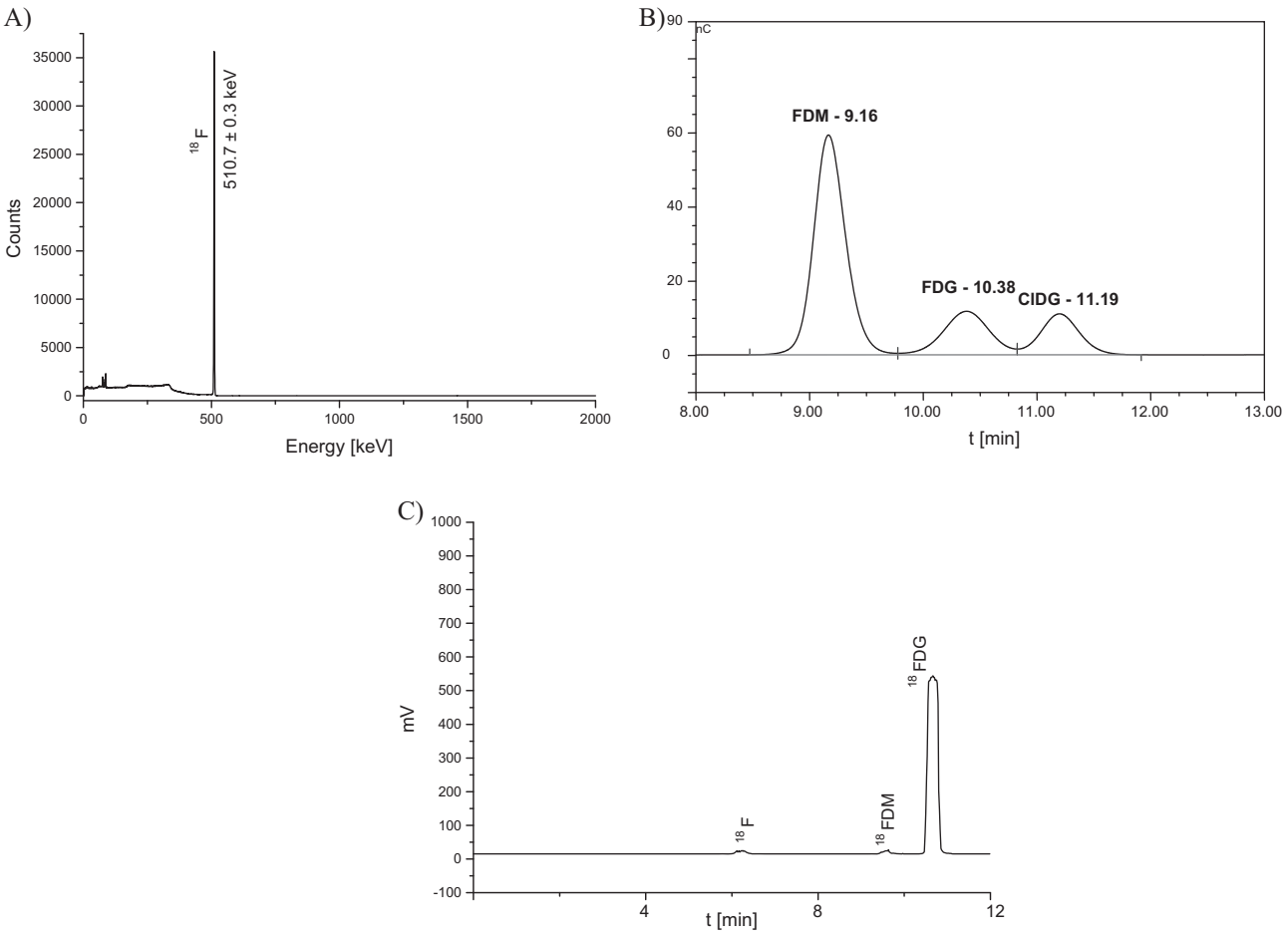

Fig. 1 – Identification of ^{18}FDG. (A) γ spectra with ^{18}F principal peak; (B) chromatogram of reference solutions. Elution order: FDM (t_r = 9.16 min), FDG (t_r = 10.38 min), ClDG (t_r = 11.19 min).

Fe, Pb, Ag, Co, Mn, Cd, Zn, Cr in ^{18}FDG and enriched water samples. Calibration curves in the range of up to 100 μg/L with four transitive points were prepared. The internal standard, ^{103}Rh was used for minimizing interferences.

3.7. *Chemicals*

Methanol, ethanol and acetonitrile used for experiment were GC grade and received from Merck. Water used for dilution was provided from validated MilliQ system and controlled for the content of organic impurities.

4. Results

4.1. *Identification*

^{18}F was identified by recording the principal γ-peak at 510 ± 0.3 keV (Fig. 1a) and determination of half-life (108.8 ± 0.9 min). ^{18}FDG was confirmed, comparing the retention times of standards, observed in the reference chromatogram with retention time of the principal signal in the radiochromatogram (Fig. 1b and c). Recorded retention times were 10.38 min for the standard and 10.55 min for the principal peak.

4.2. *Radionuclidic purity*

Gamma spectrum recorded for identification was used for determination of radionuclidic purity. Presence of any peaks with an energy different from 511 keV was checked and, except signals coming from Pb-X-rays (range 70–80 keV), none was found. That confirmed a better than 99.9% radionuclidic purity. Then ^{18}FDG sample was left for 24 h to decay the fluorine and again impurities were tested with no significant peaks, except traces of ^{18}F. Only about 2 Bq signals of ^{51}Cr, ^{52}Mn and ^{56}Co were observed, representing 10^{-8}% of total ^{18}F activity. Above mentioned results complied with radionuclidic purity tests A and B.[9] Similar levels of radionuclidic impurities were reported in other papers.[12,13,15] When impurities were not found, theoretical content was calculated by the determination of minimum detectable activities for all radionuclidic impurities found in the previous steps of the production. The activity was estimated to 3 kBq.[12]

More detailed study was conducted on radionuclidic impurities distribution along the production process with

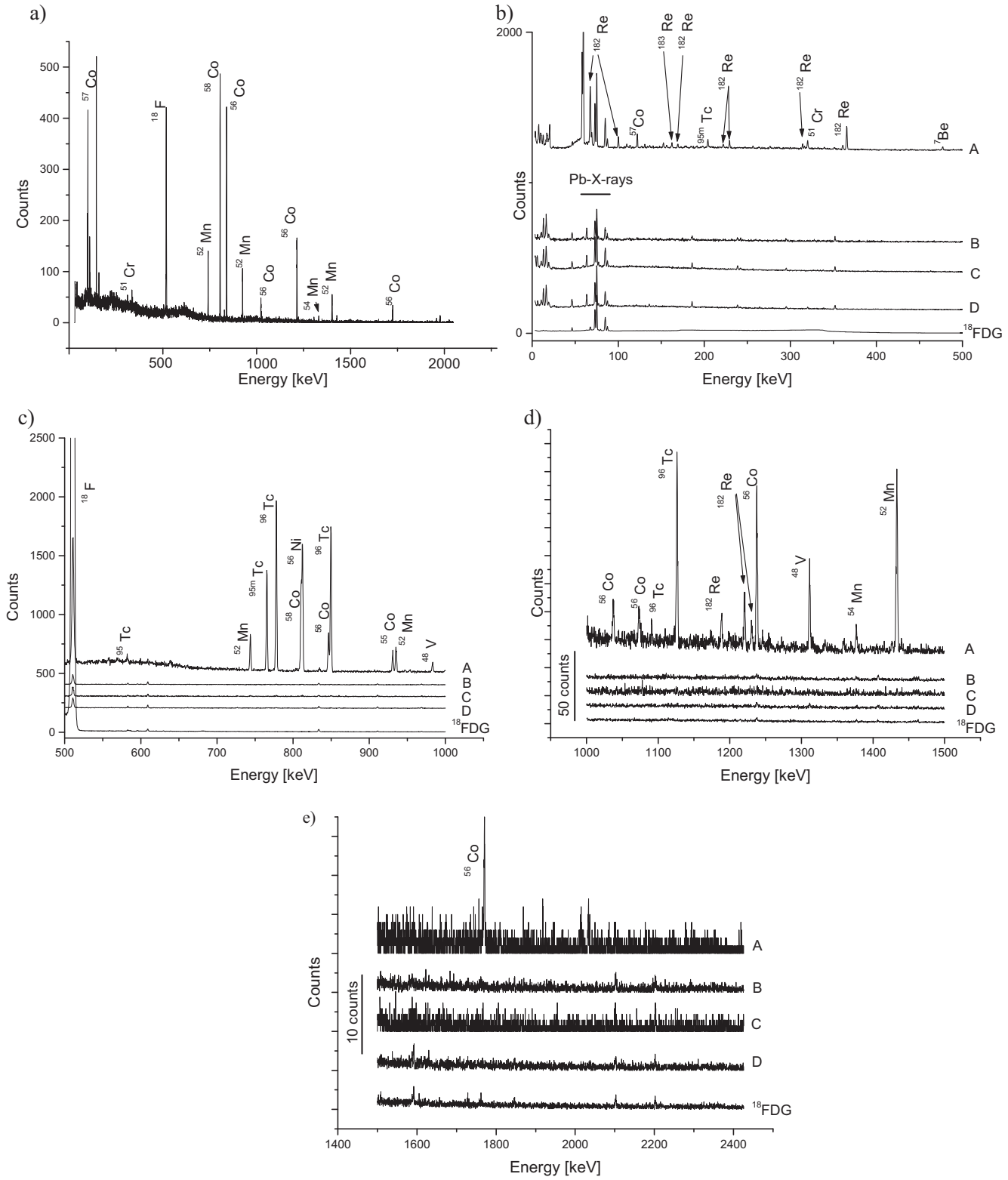

Fig. 2 – γ spectra with Ge-detector. (a) Recovery $^{18}H_2O$. QMA column (A) first C18 purification column (B), alumina purification column (C), C18 final purification column (D), final product (^{18}FDG) in the energy range: to (b) 500 keV, (c) 500–1000 keV, (d) 1000–1500 keV, and (e) 1500–2500 keV.

high resolution γ-spectrometry. Radionuclidic impurities were evaluated 72 h post-irradiation to remove dominating ^{18}F and ^{13}N by decay. It leaves out as well very short half-life (in the order up to tens of minutes) or metastable impurities, generated from target body and foils during the bombardment, covering, but not restricted to ^{50,52m}Mn, ^{60,62}Cu, ^{54}Co and technetium (^{92,94m}Tc).

Samples from the production process: of irradiated water (500 μL), ion exchange columns Accel Plus QMA Sep-PakTM, reverse phase separation columns Sep-PakTM C-18 RP used in the basic hydrolysis, the same column type used for purification process of FDG and alumina columns Sep-PakTM N Plus were used to identify radionuclides and their distribution in ^{18}FDG routine production (Fig. 2). List of identified radionuclides, their content in the recovered ^{18}O water and columns along the synthesis process are collected in Table 1.

The main source of radionuclide impurities in ^{18}FDG production is proton beam and secondary neutrons interactions with Havar® foil, containing Co (42.5%), Cr (20%), Mn (1.6%), Mo (2%), Ni (13%), W (2.8%), Fe (18.1%) and traces of carbon. Theoretical investigation showed 627 nuclear reactions possible[13] but practical results limited the number of isotopes to principal radionuclides and primary proton beam interaction. As dominating, (p,n) reactions on naturally occurring isotopes are generally proposed[12,14,16,22] with (p,α)[12,16,22] and (n,α), (n,γ)[22] supplementary paths.

The set of isotopes agreed in literature consists of ^{52}Mn, ^{54}Mn, ^{56}Co, ^{57}Co, ^{58}Co, ^{96}Tc, ^{183}Re and these isotopes are the main contributors to activity captured in foil and radiochemistry setup. Some isotopes are hardware fingerprints: ^{109}Cd for silver targets, ^{48}V in niobium target systems with titanium foils.[15] Distribution of other radionuclides was highly variable and depended on production parameters (target, proton energy and beam current), examined samples (foils, disposable cassettes, wastes, final product) and methodology of determination (equipment, time elapsed from end of bombardment (EOB) to measurement).

In this work 15 radioisotopes were identified in the QMA column. Aside from those mentioned above, ^{7}Be, ^{51}Cr, ^{55}Co, ^{56}Ni, ^{95m}Tc, ^{182}Re, ^{186} Re were found. ^{96}Tc, ^{56}Co and ^{56}Ni were the main contributors of residual activity with 70% share in total column activity (3.120 MBq). Only 6 isotopes were found in ^{18}O water after passing the QMA: ^{51}Cr, ^{52}Mn, ^{54}Mn, ^{56}Co, ^{57}Co, ^{58}Co with domination of ^{58}Co and significant contribution from ^{52}Mn, ^{56}Co and ^{57}Co. Tc and Re isotopes were not observed, which could be easily explained by chemical properties, where negatively charged perrhenate and pertechnetate ions are immobilized on QMA cartridge (Fig. 3). Activity of ^{18}Owater was 1.400 MBq (44% of QMA, 30% total activity) but individual activities of dominating isotopes were higher than in the QMA column, due to the formation of Mn and Co cationic complexes. Presence of these isotopes in QMA, which is an anionic exchanger, can be explained by the formation of hydroxycomplexes in close to neutral pH. A similar pattern and distribution (10% of activity in ^{18}O water, ca. 85% trapped in QMA) were observed in Ref. 12, but reversed proportions were found in Ref. 15, confirming high variability in impurities distribution. In this work ^{51}Cr was mainly trapped in QMA but was found as well in ^{18}O water, with traces migrating along the production path. This could be related to complex chromium equilibria in water and organic solvents and thus the distribution inconsistency was observed as in other papers.

Table 2 – Review of reported radionuclidic impurities in the recovered ^{18}O water and columns along the ^{18}FDG synthesis process.

Radionuclide	[12]	[13]	[15]	[22]	This work
^{7}Be					•
^{48}V	•				•
^{51}Cr	•		•	•	•
^{52}Mn	•	•	•	•	•
^{54}Mn	•			•	•
^{55}Co	•	•			•
^{55}Fe		•			
^{56}Co	•	•	•	•	•
^{56}Mn	•				
^{56}Ni					•
^{57}Co	•	•	•	•	•
^{57}Ni	•				
^{58}Co	•	•	•	•	•
^{59}Ni		•			
^{95}Tc	•			•	
^{95m}Tc	•		•	•	•
^{96}Tc	•	•	•	•	•
^{98}Tc	•				
^{181}Re	•				
^{182}Re	•			•	•
^{182m}Re	•		•		
^{183}Re	•		•	•	•
^{184}Re	•				
^{186}Re	•				
Total	20	10	9	11	14
Radionuclides specific for silver targets					
^{105}Ag	•				
^{106m}Ag	•				
^{109}Cd	•		•	•	

Interesting was the peak identified at the energy of 477.606 keV which corresponded to ^{7}Be. The isotope was identified only in Ref. 23 without any hypothesis about its origin. In another paper,[22] the ^{7}Be occurrence was explained by proton bombardment of trace amounts of ^{12}C, present in the Havar foil. The reaction ^{12}C(p,3n3p)^{7}Be was proposed as a source of ^{7}Be, but requires relatively high, for PET cyclotrons, proton energies. Anyhow, in this case ^{7}Be should have been observed by other authors (Table 2).

Reasonable source of ^{7}Be could be natural ^{10}B, found as chemical impurity in ^{18}O water[16] in reaction ^{10}B(p,α)^{7}Be. Boron is a ubiquitous element, common in environment and widespread in industry. The control of boron levels could not be efficient due to complex chemistry and numerous application in nuclear science and technology. Exact identification of the source is quite difficult, but it would explain why ^{7}Be was not detected by other authors.

The spectra of the other purification columns (carbon and aluminum) along the production process show <5 Bq peaks of ^{51}Cr, ^{52}Mn and ^{56}Co. This is a result of significant purification based on cationic and anionic properties of radiometallic impurities, where cations are collected in recovery water and anions are trapped in the QMA column. Residual radionuclidic impurities are separated and collected in further purification steps, resulting in that only ^{51}Cr, ^{52}Mn and ^{56}Co with activity in the range of 1–2 Bq could be recorded in the final product.

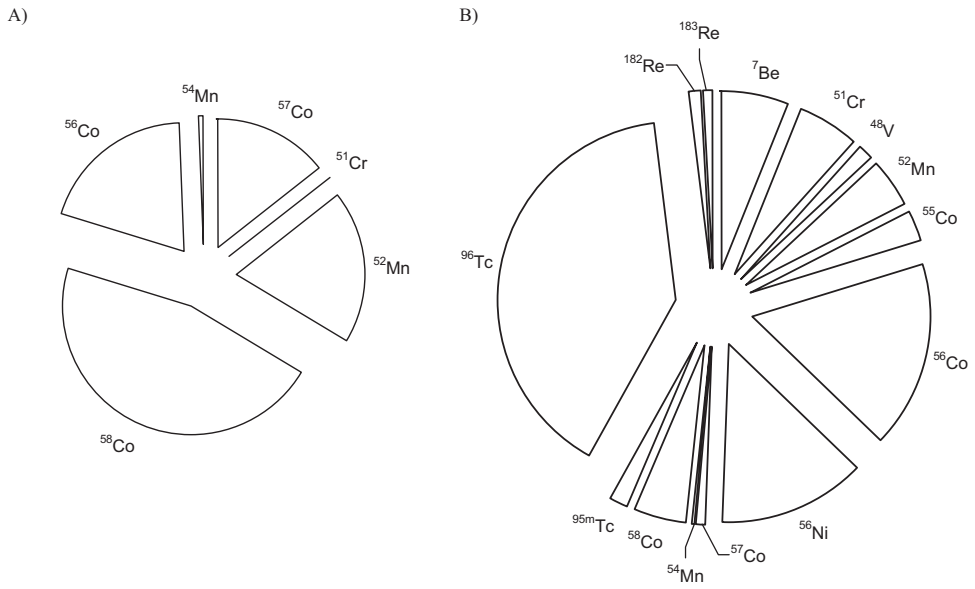

Fig. 3 – Percentage composition of activity in $^{18}H_2O$ and QMA column.

Decrease of radionuclide impurities along the production cycle was reported as in other papers,[12] as well as the radionuclide impurities produced differ depending on the target vessel materials and even when beam energy is different on the same target type. These results suggested the necessity of estimating the radionuclides produced for every combination of proton energy and ^{18}FDG unit using different target vessels.

The most notable is the remarkable reduction of chemical and radionuclidic impurities when using the Nb-sputtered Havar foil as compared with the impurities generated when using a straight Havar foil. Radiometallic impurities were decreased 10–25 times.[16] It did not influence patients' safety, because the majority of contaminants were excluded from the production process but a 6.4 percent increase in the average ^{18}FDG yield was observed.[17]

Another isotope, which has to be taken into consideration is β emitting ^{3}H from ^{18}O(p,^{3}H)^{16}O reaction. But other works verified that ^{3}H is not detected in the final product and patients receiving ^{18}FDG do not receive any extra internal exposure from tritium.[15,18]

Concluding, all impurities were efficiently eliminated from the final product and met radionuclidic purity set in Ref. 9.

5. Radiochemical purity

5.1. *Radiochemical purity was determined in all produced ^{18}FDG samples*

2-chloro-2-deoxy-D-glucose (ClDG, impurity A), ^{18}FDG and 2-^{18}fluoro-2-deoxy-mannose (^{18}FDM) were identified by ion chromatography by a qualitative comparison with the reference solution, containing maximum available concentration of ClDG, FDG and FDM and determined quantitatively from 6-points calibration curves for each standard. The retention times were 9.16, 10.38 and 11.19 min, respectively, which corresponded to relative retention factors vs. FDG: 0.88 for FDM and 1.08 for ClDG. Although the regulation for ClDG requests only pass/fail criteria, the quantitative measurements were done and average value did not exceed 0.026 mg/V (limit 0.5 mg/V). ^{18}FDG and ^{18}FDM were determined by HPLC with radiometric detection, where the principal peak of ^{18}FDG was observed at 10.55 min, with ^{18}FDM signal at 9.40 min and residual ^{18}F at 6.2 min (Fig. 1c). The average content of ^{18}FDM was 0.49%.

Six consecutive runs were analyzed in triplicate each. Free fluoride-18 ($R_f = 0.0$), ^{18}FDG ($R_f = 0.55$) and acylated-^{18}FDG ($R_f > 0.85$) were determined quantitatively. Typical radiochromatogram is presented in Fig. 4. Average content of ^{18}FDG was 96.80 ± 0.44%, with the lowest result 96.01% and >95% required in Pharmacopeia. Average content of impurities was 3.2% ± 0.44%.

5.2. *Residual organic solvents*

Organic solvents were determined with headspace gas chromatography (HS-GC). In all samples acetonitrile and ethanol were determined quantitatively, with traces of methanol observed in some samples. For the determination, originally developed method was used, where the separation of organic solvents was completed in 1 min (Fig. 5) with total time of analysis below 4 min, where the pharmacopoeial method or procedures described in literature require about 20 min for a complete separation alone. Detailed results are presented in Table 3.

The values are comparable to other formulations[19,20] which are not fortified with ethanol. To check the quality of measurements, three ^{18}F-FDG batches, available on the market, were analyzed in parallel with manufacturer's laboratory, working as commercial ^{18}F-FDG provider, using a standard Ph.Eur. method, with 20 min of chromatographic separation. The results are presented in Table 4 and show good correlation. However, our proposed method has a better limit of detection and throughput of samples.

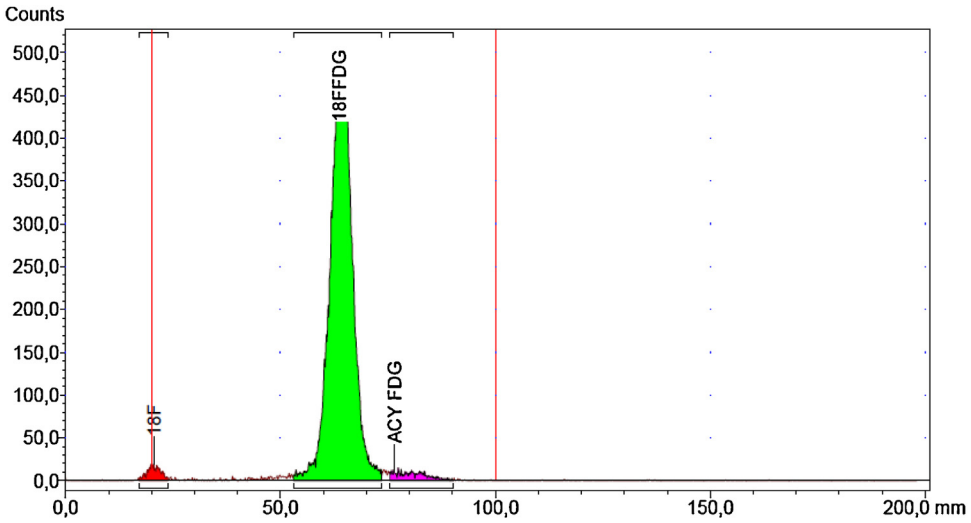

Fig. 4 – TLC radiochromatogram of ^{18}FDG sample.

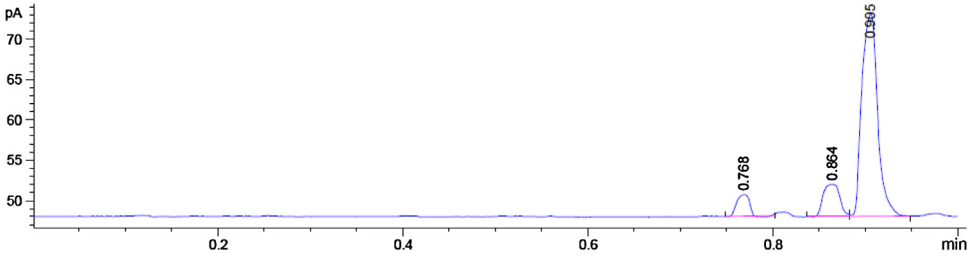

Fig. 5 – Chromatogram of residual solvents in ^{18}FDG. Elution order: methanol, ethanol, acetonitrile.

Table 3 – Determined QC parameters in ^{18}F-FDG. Acceptance criteria according to Ref. 9. IU/V: endotoxins unit per recommended dose in mL; mg/V: milligrams per recommended dose in mL.

Determined values in $n = 6$ consecutive runs		
Parameter	Acceptance criteria	Value
Identification	Principal peak 511 keV Half-life 105–115 min CRS FDG t_r = 10.38 min	510.7 ± 0.3 keV 108.8 ± 0.9 min ^{18}FDG t_r = 10.55 min
pH	4.5–8.5	6.24–6.75
Radiochemical purity	^{18}FDG + ^{18}FDM > 95% ^{18}FDM < 10% FDG < 0.5 mg/V ClDG < 0.5 mg/V TLC ^{18}FDG > 95% Kryptofix < 2.2 mg/V	98.4 ± 0.8 0.49 ± 0.13 Pass Pass 98.6 ± 0.6% Pass
Osmolality	280–310 mOsm	293 ± 14 mOsm
Residual solvents	Ethanol < 5000 mg/kg Acetonitrile < 4.10 mg/V	29 ± 1 mg/kg 0.77 ± 0.03 mg/V
Sterility	Sterile	Pass
Bacterial endotoxin test	<175/V IU/mL	Pass
Radionuclidic purity test A	511 keV > 99.9%	Pass
Radionuclidic purity test B	Impurities < 0.1%	Pass

Table 4 – Comparison of the results with the reference laboratory[a] for the determination of residual solvents in different batches of ^{18}F-FDG, manufactured by commercial supplier.

	This method		Batch 1		Batch 2		Batch 3	
	LOQ (mg/L)	Precision (%) ($n=6$)	Reference lab (mg/L)	This method (mg/L)	Reference lab (mg/L)	This method (mg/L)	Reference lab (mg/L)	This method (mg/L)
Methanol	3	6.1	N/A	<3	N/A	<3	N/A	<3
Ethanol	3	6.8	<35	23.1	<35	10.6	164	170.1
Acetonitrile	0.4	3.9	<31	5.9	<31	5.6	<31	6.3

LOQ: limit of quantification.
[a] The reference laboratory supplies commercially available ^{18}F-FDG and uses the standard Ph.Eur. method.

Table 5 – Heavy metals content in recovery water and 18FDG samples. EMEA guidelines[21] parenteral limit.

	LOQ [μg/L]	Recovery water [μg/L]	^{18}FDG [μg/L]	EMEA guidelines limits [μg/L]
Cu	0.09	1.63 ± 0.09	4.6 ± 0.4	5000
Fe	21	<LOQ	<LOQ	150
Pb	0.13	14.7 ± 1.3	0.42 ± 0.18	100
Ag	0.18	19.0 ± 0.9	<LOQ	N/A
Co	0.11	5.2 ± 0.1	<LOQ	10,000
Mn	0.08	0.52 ± 0.04	0.48 ± 0.10	70,000
Cd	0.15	<LOQ	<LOQ	250
Zn	1.1	59 ± 3	250 ± 50	150,000
Cr	0.7	3.8 ± 0.4	27.6 ± 1.5	1500

LOQ: limit of quantification.

5.3. *Heavy metals determination*

Heavy metal content was determined in six ^{18}FDG samples and respective recovery water from each run. First, a quantitation limit was determined as an average blank $\pm$ 6 standard deviation. Then determination of 9 heavy metals: Cu, Fe, Pb, Ag, Co, Mn, Cd, Zn and Cr in samples was conducted. Summarized values of the quantitation limit are presented in Table 5. Presented results clearly indicate that the metal impurities are not a serious threat for the quality of the produced FDG and are significantly lower than set by the regulatory office.[21] Most of the metallic impurities are concentrated in the ion exchange column in the inlet or migrate with enriched water to recovery and do not influence significantly the synthesis process. A slight increase in the concentration of copper, zinc and chromium in the final product is observed. The first two are common trace contaminants and are difficult to remove as their probable source is a saline solution used for the final formulation. Increasing concentration of chromium can be explained by the presence of elements of stainless steel in the dispensing line.

Isotonicity, pH, Kryptofix content, sterility and endotoxin test, as generally known procedures are summarized in Table 3. All parameters were according to the quality criteria for ^{18}FDG.

6. Conclusions

All of the impurities were efficiently determined and then eliminated in the ^{18}FDG synthesis process, and the final product was purified from main radionuclidic and metallic impurities. Final product meets the requirements set by relevant regulations.

Conflict of interest

None declared.

Financial disclosure

None declared.

REFERENCES

1. Hoh CK. Clinical use of FDG PET. *Nucl Med Biol* 2007;**34**:737–42.
2. Lobert P, Brown RKJ, Dvorak RA, Corbett JR, Kazerooni EA, Wong KK. Spectrum of physiological and pathological cardiac and pericardial uptake of FDG in oncology PET-CT. *Clin Radiol* 2013;**68**:e59–71.
3. Wang Z, Chen JQ, Liu JL, Qin XG, Huang Y. FDG-PET in diagnosis, staging and prognosis of pancreatic carcinoma: a meta-analysis. *World J Gastroenterol* 2013;**19**(August (29)):4808–17.
4. Seth R, Puri K, Singh P, Selvam P, Kumar R. The role of fluorodeoxyglucose positron emission tomography-computerized tomography in resolving therapeutic dilemmas in pediatric Hodgkin lymphoma.,. *Indian J Nucl Med* 2012;**27**(July (3)):141–4.
5. Kostakoglu L, Gallamini A. Interim 18F-FDG PET in Hodgkin lymphoma: would PET-adapted clinical trials lead to a paradigm shift? *J Nucl Med* 2013;**54**(July (7)):1082–93.
6. Quartuccio N, Treglia G, Salsano M, et al. The role of fluorine-18-fluorodeoxyglucose positron emission tomography in staging and restaging of patients with osteosarcoma. *Radiol Oncol* 2013;**47**(May (2)):97–102.
7. Siva S, Byrne K, Seel M, et al. ^{18}F-FDG PET provides high-impact and powerful prognostic stratification in the

staging of Merkel cell carcinoma: a 15-year institutional experience. *J Nucl Med* 2013;**54**(August (8)):1223–9.
8. Perea BC, Villegas AC, Rodríguez JMD, Velloso MJG, Vic AMG. Recommendations of the Spanish Societies of Radiation Oncology (SEOR), Nuclear Medicine & Molecular Imaging (SEMNiM), and Medical Physics (SEFM) on 18F-FDG PET-CT for radiotherapy treatment planning. *Rep Prac Oncol Radiother* 2012;**17**:298–318.
9. European Pharmacopoeia 8th Edition 2013.
10. Fuchtner F, Steinbach J, Madin P, Johannsen B. Basic hydrolysis of 2-[^{18}F]fluoro-2,3,4,6-tetra-O-acetyl-D-glucose in the preparation of 2-[^{18}F]fluoro-deoxy-D-glucose. *Appl Radiat Isot* 1996;**47**:61–6.
11. Mock B, Winle W, Vavrek MT. A color spot test for the detection of kryptofix 2.2.2 in [^{18}F]FDG preparations. *Nucl Med Biol* 1997;**24**:193–5.
12. Marengo M, Lodi F, Magi S, Cicoria G, Pancaldi D, Boschi S. Assessment of radionuclidic impurities in 2-[^{18}F]fluoro-2-deoxy-D-glucose ([^{18}F]FDG) routine production. *Appl Radiat Isot* 2008;**66**(March (3)):295–302.
13. Ito S, Sakane H, Deji S, Saze T, Nishizama K. Radioactive byproducts in [^{18}O]H_2O used to produce ^{18}F for[^{18}F]FDG synthesis. *Appl Radiat Isot* 2006;**64**:298–305.
14. Mochizuki S, Ishigure N, Ogata Y, Kobayashi T. Analysis of induced radionuclides in replacement parts and liquid wastes in a medical cyclotron solely used for production of ^{18}F for [^{18}F]FDG. *Appl Radiat Isot* 2013;**74**(April):137–43.
15. Bowden L, Vintró LL, Mitchell PI, O'Donnell RG, Seymour AM, Duffy GJ. Radionuclide impurities in proton-irradiated [^{18}O]H_2O for the production of ^{18}F-: activities and distribution in the [^{18}F]FDG synthesis process. *Appl Radiat Isot* 2009;**67**(February (2)):248–55.
16. Avila-Rodriguez MA, Wilson JS, McQuarrie SA. A quantitative and comparative study of radionuclidic and chemical impurities in water samples irradiated in a niobium target with Havar vs. niobium-sputtered Havar as entrance foils. *Appl Radiat Isot* 2008;**66**(December (12)):1775–80.
17. Gagnon K, Wilson JS, Sant E, Backhouse CJ, McQuarrie SA. Assessing the performance and longevity of Nb, Pt, Ta, Ti, Zr, and ZrO_2-sputtered Havar foils for the high-power production of reactive [^{18}F]F by proton irradiation of [^{18}O]H_2O. *Appl Radiat Isot* 2011;**69**(October (10)):1330–6.
18. Ito S, Saze T, Sakane H, Ito S, Ito S, Nishizawa K. Tritium in [^{18}O]water containing [^{18}F]fluoride for [^{18}F]FDG synthesis. *Appl Radiat Isot* 2004;**61**(December (6)):1179–83.
19. Koziorowski J. A simple method for the quality control of ^{18}FDG. *Appl Radiat Isot* 2010;**68**:1740–2.
20. Channing MA, Huang BX, Eckelman WC. Analysis of residual solvents in 2-[^{18}F]FDG by GC. *Nucl Med Biol* 2001;**28**:469–71.
21. *Guideline on the specification limits for residues of metal catalysts or metal reagents, EMEA/CHMP/SWP/4446/2000, London, 21 February*; 2008.
22. Ferguson D, Orr P, Gillanders J, Corrigan G, Marshall C. Measurement of long lived radioactive impurities retained in the disposable cassettes on the Tracerlab MX system during the production of [^{18}F]FDG. *Appl Radiat Isot* 2011;**69**: 1479–85.
23. Gillies JM, Najima N, Zweit J. Analysis of metal radioisotope impurities generated in [^{18}O]H_2O during the cyclotron production of fluorine-18. *Appl Radiat Isot* 2006;**64**:431–4.